Journal of Applied Polymer Science

Influence of the solvent and nonsolvent composition on the electrospinning of a cellulose acetate ternary system

Reza Korehei,[1] James Olson,[1] Frank Ko,[2] John Kadla[3]

[1]Department of Mechanical Engineering, University of British Columbia, 6250 Applied Science Lane, Vancouver, British Columbia V6T1Z4, Canada

[2]Department of Materials Engineering, University of British Columbia, 2355 East Mall, Vancouver, British Columbia V6T 1Z4, Canada

[3]Department of Forest Biomaterials, North Carolina State University, Raleigh, North Carolina 27695

Correspondence to: J. Kadla (E-mail: john.kadla@shaw.ca)

ABSTRACT: A series of cellulose acetate (CA) ternary system solutions consisting of the CA, *N*,*N*-dimethylacetamide, and various nonsolvents, such as 1-propanol, 1-hexanol, 1-octanol, 1-decanol, 1,3-propane diol, and glycerol, were prepared, and the effects of the component composition on the solutions characteristics and electrospinning were examined. In particular, the effects of the nonsolvent concentration, structure, and degree of miscibility with other components were studied. In some cases, increasing the nonsolvent content increased the solution viscosity and facilitated the electrospinning process. However, we found that electrospinning was also governed by the structure of the nonsolvents and by the solution viscosity. An increase in the number of hydroxyl groups or an increase in the hydrocarbon chain length of the monohydroxyl alcohol nonsolvent improved the fiber formation. The calculated Hansen sphere [$D_{(S\text{-}p)}$] values of the CA ternary system solution were then used to explain their electrospinnability. The increases in the hydrophilicity and hydrophobicity of system caused by changes in the nonsolvent structure increased the $D_{(S\text{-}p)}$ values and improved fiber formation in electrospinning process. The calculated $D_{(S\text{-}p)}$ values were also shown to be in good agreement with the obtained microscopy images of the electrospun fiber. © 2015 Wiley Periodicals, Inc. J. Appl. Polym. Sci. **2015**, *132*, 42819.

KEYWORDS: cellulose and other wood products; electrospinning; fibers; rheology

Received 24 February 2015; accepted 4 August 2015

DOI: 10.1002/app.42819

INTRODUCTION

Cellulose acetate (CA) is one of the most important and commercially relevant renewable polymers, and it is used in a number of different industries.[1] In particular, CA is widely used in the manufacturing of separation and filtration media.[2] Because of its hydrophilic nature, low binding attraction, and biocompatibility, CA membranes are suitable for maximum sample recovery during tissue culture media preparation, and the sterile filtration of biological fluids, proteins, enzymes, and many other biological components.[2–6] Depending on the application, the optimal permeability of the CA membrane can be obtained by the adjustment of the pores sizes from nanometer to micrometer diameter.[7] The CA membranes with various pore sizes could be fabricated through the use of different solidification or gelation processes, such as nonsolvent-induced phase separation, reversible thermal gelation, coagulation, or immersion precipitation and electrospinning.[7–11]

Recently we showed that the gelation of CA could be achieved by the addition of various alcohols as nonsolvents to CA/*N*,*N*-dimethylacetamide (DMA) solutions.[7,12] In these systems, the physical gelation of CA arose as a result of phase separation induced by the addition of the nonsolvent to the CA ternary system. The gelation point of CA was shown to be highly dependent on the nonsolvent concentration and structure. Microscopic images of the solid CA network exhibited a microstructure of solid packing with uniform pore sizes, which were dependent on the nonsolvent structure and concentration used. In that study, CA membranes were produced via a wet-phase inversion method. Because the alcohols used were weak CA coagulants or quenching media, high nonsolvent additions were required to form the CA membrane microstructures.

Another way to produce CA membranes or nonwoven CA fibrous microstructure is via electrospinning. Electrospinning is a reliable method for producing uniform micrometer/nanosized

Additional Supporting Information may be found in the online version of this article.

fibers from polymer solutions, wherein a three-dimensional membrane filter can ultimately be obtained.[13–15] CA fibrous membranes have been widely studied and generated via the electrospinning process.[16–20] It is evident that the choice of cosolvents and additives can exhibit dramatic effects on the CA electrospinning process. Mixed random solvents systems, such as acetone/water, acetic acid/water, DMA/acetone, acetone/dimethylformamide (DMF), DMF/trifluoroethylene, chloroform/methanol, and dichloromethane/methanol, have been used to produce CA electrospun fibers.[3,21–23] Although these CA fibers have been prepared from systems with mixed solvents, an organized approach has not been conducted to investigate the effects of solvent/nonsolvent systems on CA fiber formation. In this study, a systematic approach was used to study the effects of various mixed solvent/nonsolvent systems on the CA solution properties and the resulting electrospun fiber morphology. Alcohols were used as nonsolvents to increase the hydrophobicity and hydrophilicity of the ternary system by increasing the alkyl chain lengths of monohydroxyl alcohols [1-propanol (Pro), 1-hexanol (Hex), 1-octanol (Oct), and 1-decanol (Dec)] or by increasing the number of hydroxyl groups of the same alkyl length [Pro, 1,3-propane diol (PD), and glycerol (Gly)]. Here, the effects of the alcohol structures on the solution properties and the resulting electrospun fibers were investigated. Consideration was also given to other important functional parameters, such as the Hansen solubility and the Flory–Huggins values, to better understand the phase separation and fiber formation of CA in the ternary systems.

EXPERIMENTAL

Materials

CA (number-average molecular weight ≈ 30,000 g/mol, degree of acetylation = 2.45), DMA (high-performance liquid chromatography (HPLC) grade), Pro, Hex, Oct, Dec, PD, and Gly were purchased from Sigma-Aldrich and were used as received.

Preparation of the CA Ternary Solutions

The first step in the preparation of the various CA systems was to prepare a bulk CA/DMA (28.12 wt %) solution. To facilitate mixing and to produce a homogeneous solution, the CA/DMA mechanical mixture was heated in an oven at 100°C for 20 min. The various ternary systems were then prepared through the addition of a specific amount of nonsolvent (monohydric, dihydric, and trihydric alcohols, which were prepared as DMA solutions at nonsolvent concentrations that varied from 26.6 to 53.3 wt %). Three CA concentrations were prepared: 10, 15, and 20 wt %. To ensure complete miscibility and the elimination of air bubbles, the samples were manually mixed and heated for 10–15 min at 100°C. All of the samples were prepared in 15-mL glass scintillation vials (Fischer Scientific, Fisher brand). All of the samples were equilibrated for exactly 1 week in a desiccator at room temperature before analysis. All of the solutions and dilutions were prepared on a weight basis.

CA Solution Characterization

A TA Instruments advanced rheometer (AR 2000) was used to measure the viscosity (η) of the samples. In a typical experiment, 4 mL of CA solution (excess sample) was loaded onto the center of the bottom plate. The upper geometry (60-mm diameter, 2° cone) was lowered to the adjusted zero gap, and the excess solution around the geometry was removed. The solutions were then relaxed for 1 min to reach an equilibrium state before η measurement. We performed steady shear measurements by subjecting the sample to a steady shear at a constant shear rate (γ); this resulted in the generation of a shear stress. The corresponding shear stress was measured with a torque transducer. η was measured as a function of the steady γ. The γ values ranged from 0.05 to 500 s^{-1}. All analyses were performed at ambient temperature (25°C). The surface tension of the CA ternary system solutions were measured with an interfacial tension meter (Kruss model K14) at 20°C via the plate method, and the conductivities were measured by a conductivity meter (Isteck model 455C) at 20°C.

Electrospinning

Electrospinning was performed in a vertical orientation inside a glass box under controlled processing conditions at a 24°C laboratory temperature and a 35% relative humidity. For all of the electrospinning experiments, the CA ternary solution was placed in a 10-mL syringe attached to flat-tip needle (18 gauge, 2 cm long), which was positioned above a grounded metallic collector. The positive electrode of a high-voltage power supply (FC30P4, Glassman High Voltage, Inc.) was connected with a copper wire to the needle of a syringe containing the CA solution. The distance from the tip of the needle to the collector was 15 cm, and the applied voltage was set at 15 kV (1 kV/cm). The CA nanofibrous mats were obtained on the metallic collector and dried *in vacuo* for 24 h to remove any trace solvent.

Microscope Analysis

The morphology of the electrospun fibers was examined with a Hitachi S-2600N scanning electron microscope. The scanning electron microscopy (SEM) samples were prepared by the direct electrospinning the fibers onto an aluminum SEM stub and were subsequently imaged with an operating voltage of 25 kV and a working distance of 10 mm. Images were taken from duplicate samples over a magnification range of 250–4000×. Before imaging, the samples were quickly frozen, lyophilized, and sputter-coated with a Cressington high-resolution sputter coater *in vacuo* between 0.04 and 0.03 Torr for 3 min until the fiber samples were covered with a thin layer of Au (5 nm).

Fourier Transform Infrared (FTIR) Spectroscopy

FTIR spectra were measured on a PerkinElmer 16PG FTIR spectrometer. A total of 16 scans were collected at a resolution of 4 cm^{-1} over a range of 400–4000 cm^{-1} with 10-mg samples positioned between ZnSe salt plates. Care was taken not to disrupt the sample microstructure during the transfer while they were being positioned between the plates.

Data Analysis

We determined the experimental error by running multiple samples (minimum of three samples) for all of the different electrospinning systems and their characterization. In this study, all of the raw data presented are the averages of the replicate runs, and the difference between the highest and lowest values was less than 5%. This was consistently the case for all of the experimental measurements.

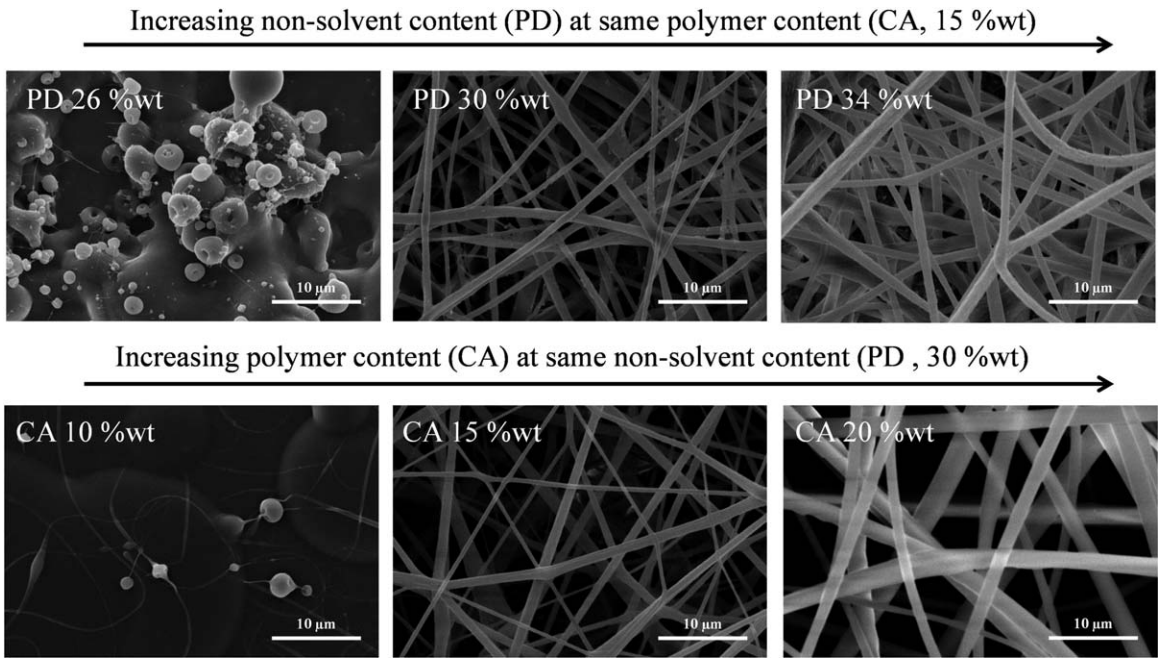

Figure 1. Effects of the nonsolvent and polymer contents on the electrospinning process and fiber morphology of the CA ternary system.

RESULTS AND DISCUSSION

Effects of the Nonsolvent Content on CA Electrospinning

In a previous study, we showed that the addition of alcohol to a CA/DMA solution led to an increase in solution η (Figures S1 and S2, see Supporting Information).[7,12] At a critical nonsolvent content, phase separation was observed, and the sample exhibited a high shear η followed by gelation or the formation of a solid three-dimensional network structure (Figures S3–S5, see Supporting Information). Both CA and the nonsolvent concentration and structure affected the gelation process and resulting gel/sol microstructure. The effect of hydrophilic and hydrophobic interactions on the solution behavior of the CA/DMA/nonsolvent ternary system were investigated through changes in the nonsolvent structure. The effects of hydrophilic interactions, specifically hydrogen bonding, propyl alcohols with various numbers of hydroxyl groups, that is, Pro, PD, and Gly (1,2,3-propane triol), were investigated. Likewise, we studied the effects of the hydrophobic interactions on the gel behavior by manipulating the hydrophobicity of the systems by increasing the alkyl chain length of the monohydric alcohols from Hex to Oct to Dec (Figure S7).

To investigate the impact of the solvent/nonsolvent interactions on CA fiber formation, the various CA ternary solutions were subjected to electrospinning. First, the effects of the CA and nonsolvent contents on the electrospinning of the CA ternary system were examined. The electrospinning of the 15 wt % CA ternary systems revealed distinct results from various monohydric and poly(hydroxyl alcohol)s as nonsolvents in the systems. Changes in the nonsolvent structure from monohydroxyl alcohol to dihyroxyl alcohol (PD) showed the largest change in the electrospinning process; CA ternary systems containing PD alcohol were chosen as a system to demonstrate the effect of the nonsolvent content on the CA fiber formation. Figure 1 shows SEM micrographs of the CA electrospun fibers produced at three different PD content levels. The electrospinning process at low PD contents ($\leq$23 wt %) mainly resulted in spraying, with limited fiber formation between large droplets (Figure 1, top left). An increase in the PD content to 30 wt % led to a continuous electrospinning process and the formation of CA fibers with an average diameter of less than 1.0 μm (Figure 1, top middle). A further increase in the PD content to 36 wt % enhanced the fiber diameter to more than 1.5 μm (Figure 1, top right).

As expected, the electrospinning of the CA ternary system was also shown to be effected by the CA concentration. At a low CA content (10 wt %), the electrospinning process failed to produce

Table I. Effect of the PD Content on the Solution Properties of the CA/DMA/PD Ternary System

Ternary system	Surface tension (dyn/cm)	Conductivity (μs/cm)	η (Pa s)[a]
CA (15%)/DMA	43.0	4.26	1.24
CA (15%)/DMA/PD (24%)	46.0	2.69	2.9
CA (15%)/DMA/PD (30%)	48.0	2.40	6.7
CA (15%)/DMA/PD (36%)	50.0	2.13	26.1

[a] η values were taken from a steady shear η plot at a γ of 1 s^{-1}.

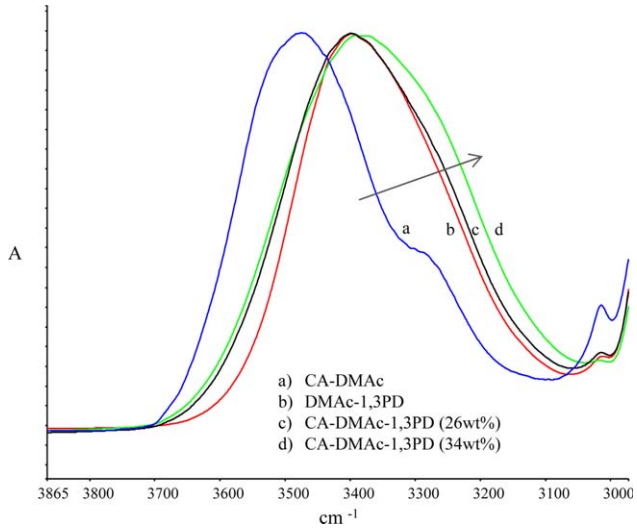

Figure 2. FTIR spectra of the hydroxyl stretching region of (a) CA/DMA, (b) DMA/PD, (c) CA/DMA/PD (26 wt %), and (d) CA/DMA/PD (34 wt %). DMAc: N, N-dimethylacetamide. [Color figure can be viewed in the online issue, which is available at wileyonlinelibrary.com.]

any fiber (Figure 1, bottom left); however, increases in the CA concentration to 15 and 20 wt %, at the same nonsolvent content (30 wt %), resulted in the formation of fibers with average diameters of 1.0 and 2.0 μm, respectively (Figure 1, bottom middle and right).

The electrospinning of CA with various solvent systems was well investigated. It is well documented that the electrospinning of CA in only DMA does not result in fiber formation because of the high surface tension and boiling point of the solvent.[21] However, the addition of acetone or chloroform reduced the surface tension of the CA/DMA solution and resulted in uniform CA electrospun fibers.[3,21,23] In general, the formation of electrospun fibers is mainly governed by the polymer solution properties, such as the solution conductivity, η, and surface tension.[11,24] In our ternary system, the addition of a nonsolvent (e.g., PD) to the CA/DMA solution was found to increase the surface tension and reduce the solution conductivity (Table I). Theoretically, this should not favor fiber formation, but interestingly, the addition of nonsolvent did facilitate electrospinning and the production of uniform CA electrospun fibers. The observed improvement in the electrospinning of the CA ternary system could have been due to the enhancement in the solution η; steady shear η measurements revealed a significant increase in the solution η through the addition of nonsolvent (Table I).

The increase in η (Table I) with increasing nonsolvent addition was likely due to an enhancement in the intermolecular hydrogen bonding formed between the components of the ternary system.[7,12] FTIR spectroscopy revealed a significant change in the hydroxyl stretching region band ($\upsilon_{OH} \approx 3700–3000\ cm^{-1}$) envelopes' shape and wave-number position upon the addition of nonsolvent (Figure 2). There were clear differences between the FTIR spectra for CA/DMA, DMA/PD, and CA/DMA/PD at different PD contents. On the basis of the band envelope shape and the wave number of the major peak, it was evident that stronger hydrogen bonds existed between DMA and the nonsolvents than between those formed with CA. Moreover, the FTIR spectrum of the CA/DMA/PD solution clearly showed the presence of very strong hydrogen bonds between CA and PD; these were significantly stronger than those between CA/DMA and DMA/PD. In addition, an increase in the nonsolvent concentration from 26 to 34 wt % further increased the intermolecular hydrogen bonding, and the hydroxyl stretching band shifted to a lower wave number. The intensification of intermolecular hydrogen bonding as a result of PD addition supported the observed η enhancement in the ternary system. Increasing the PD content formed extensive hydrogen bonding in the ternary system; this essentially acted as chain entanglements and ultimately facilitated fiber formation. This complex hydrogen-bonding network system was further magnified by increasing the CA concentration, for example, from 10 to 20 wt %, and this resulted in an increase in the electrospun fiber diameter (Figure 1).

Effect of the Nonsolvent Structure on CA Electrospinning

Increasing the nonsolvent content enhanced the intermolecular bonding and η of the ternary solution; this led to better performance in the electrospinning process. To verify the effect of intermolecular bonding on the electrospinning process, various nonsolvents with different structures were used. More specifically, the effect of the hydrophilicity and hydrophobicity on fiber formation was investigated through increases in the number of hydroxyl groups and alkyl chain length of the nonsolvent, respectively.

Table II. Effect of the Nonsolvent Structure on the Solution Properties of the CA/DMA/Nonsolvent Ternary Systems with 15 wt % CA and 30 wt % Nonsolvent Contents

Ternary system	Surface tension (dyn/cm)	Conductivity (μs/cm)	η (Pa s)
CA (15%)/DMA/Pro (30%)	34	3.43	1.5
CA (15%)/DMA/Hex (30%)	36	2.77	2.0
CA (15%)/DMA/Oct (30%)	37	2.20	2.4
CA (15%)/DMA/Dec (30%)	38	2.08	3.6
CA (15%)/DMA/PD (30%)	48	2.40	6.7
CA (15%)/DMA/Gly (30%)	50	1.50	24.2

[a] η values were taken from a steady shear η plot at a γ of 1 s^{-1}.

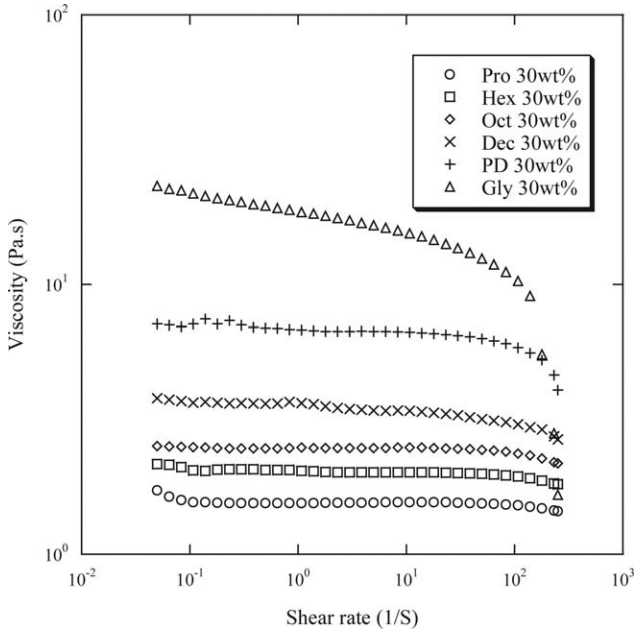

Figure 3. Effect of the nonsolvent structure on the steady η of the CA/DMA/nonsolvent system at a constant CA (15 wt %) and nonsolvent (30.0 wt %) contents.

Increasing the number of hydroxyl groups in the nonsolvent from Pro to PD to Gly increased the solution η and surface tension of the ternary system (Table II and Figure 3). Likewise, increasing the alkyl chain length of the monohydroxyl alcohol nonsolvents from 3 to 10 carbons with Pro, Hex, Oct, and Dec also enhanced the solution's η and surface tension. Although increases in the alkyl chain length of the nonsolvents enhanced η of the ternary solutions, the resulting η values were much lower than those obtained with the smaller dihydric (PD) and trihydric (Gly) alcohol nonsolvents (Table II and Figure 3). This demonstrated the significant effect of hydrophilic interactions (i.e., increasing hydroxyl groups) as opposed to hydrophobic interactions (i.e., increasing alkyl chain length monohydroxyl alcohols) on the viscoelastic properties of the ternary system.

As expected, these differences in the solution properties also affected the outcome of the electrospinning process. Increasing both the number of hydroxyl groups and alkyl chain length of the nonsolvent enhanced the electrospinning process. At the same, the nonsolvent content (30 wt %) electrospinning of the monohydroxyl alcohol nonsolvent (Pro) formed only small droplets because of spraying, whereas those obtained with the dihydroxyl (PD) and trihydroxyl (Gly) nonsolvents generated electrospun fibers with an average diameter of 1.0 and 1.5 μm, respectively (Figure 4). Here, the deficiency in fiber formation with the monohydroxyl group (Pro) could have been due to the low solution η and insufficient intermolecular interactions between the CA polymer and the small Pro molecule. However, through increases in the number of hydroxyl groups in the nonsolvent, the extent/strength of intermolecular interactions, for example, hydrogen bonding, was significantly increased and, thereby, promoted fiber formation.

Although extending the alkyl chain length (size) of the monohydroxyl alcohol nonsolvents from 3 to 10 increased the ternary systems' solution η (Table II and Figure 3) and likely the molecular chain entanglement, the viscosities were still much lower than those of the dihydroxyl and trihydroxyl alcohol ternary systems. In general, increases in the alkyl chain length (hydrophobicity) of the monohydroxyl alcohol nonsolvent (30 wt %) resulted in an overall improvement in the electrospinning process. However, as shown in Figure 4, the electrospinning of the shorter alkyl chain (Pro and Hex) ternary systems produced only small droplets. Increasing the alkyl chain length to eight carbons (Oct) generated some short fibers between a majority of droplets; this further improved to a majority of fibers when the nonsolvent alkyl chain length was increased to 10 carbons (Dec). However, despite this ternary system (CA/

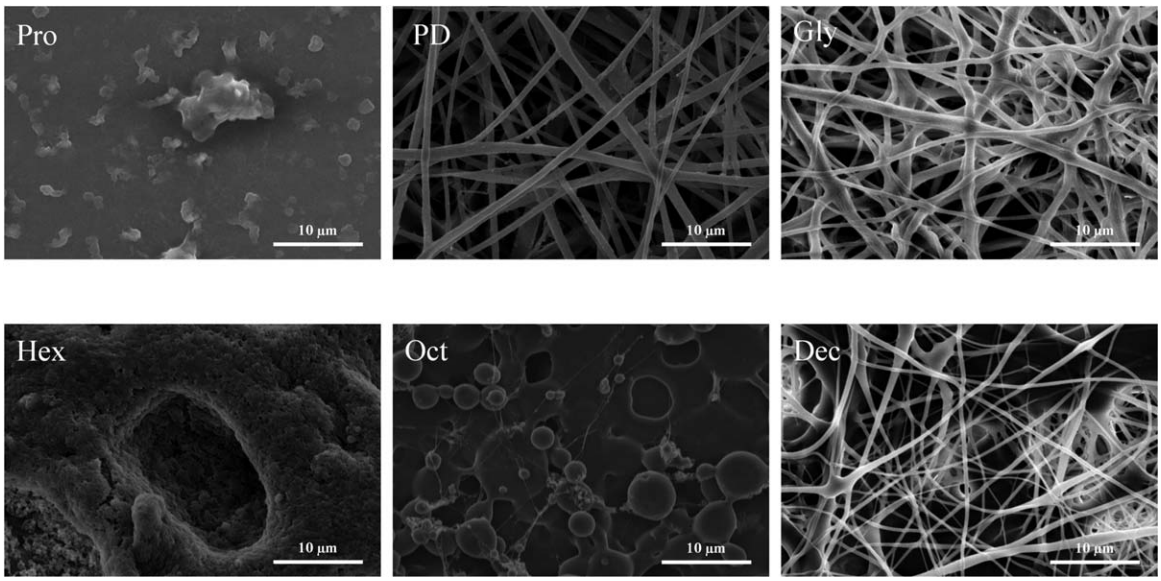

Figure 4. Effect of the nonsolvent structure on the electrospinning of CA ternary systems. The CA and nonsolvent contents were kept constant at 15 and 30 wt %, respectively.

Table III. Solution Properties of the CA Ternary Systems with Their Maximum Nonsolvent Contents[a]

Ternary system	Surface tension (dyn/cm)	Conductivity (μs/cm)	η (Pa s)[b]
CA (15%)/DMA/Pro (48.3%)	37	2.54	4.4
CA (15%)/DMA/Hex (40.0%)	38	1.69	9.6
CA (15%)/DMA/Oct (34.6%)	39	1.67	13.6
CA (15%)/DMA/Dec (31.6%)	40	1.51	32.3
CA (15%)/DMA/PD (35.0%)	49	2.22	21.6
CA (15%)/DMA/Gly (30.0%)	50	1.50	24.2

[a] Maximum nonsolvent contents before gelation/phase separation.
[b] η values were taken from a steady shear η plot at a γ of 1 s^{-1}.

DMA/Dec) resulting in a smooth electrospinning process, the SEM images revealed an inferior, stretched, beaded CA fiber morphology.

Generally, η of a solution has a profound effect on electrospinning and the resulting fiber morphology. The η of the polymer solution is mainly related to the polymer chain entanglement and/or the interaction between the polymer and other small molecules within the solution. We assumed that the deficiency in fiber formation for the ternary systems containing monohydroxyl alcohols with short alkyl chain lengths (1-Pro, 1-Hex) was due to the low solution η. Therefore, to test this hypothesis, the η values of all of the ternary systems were increased by the addition of nonsolvent to a maximum content right before gelation (Table III). At 30 wt % nonsolvent concentration, the viscosities were about 1.5, 2, 2.4, and 3.6 Pa s for Pro, Hex, Oct, and Dec, respectively (shown in Table II and Figure S5) and 6.7 and 24.2 Pa s for PD and Gly, respectively. Therefore, it appeared that in dilute solutions, hydrophilic interactions, such as hydrogen bonding, had a greater effect on η than hydrophobic interactions. The presence of more hydroxyl groups on the nonsolvent enabled increased hydrogen bonding between constituents; this led to an increase in η. However, with the addition of nonsolvent contents, η enhancement occurred very quickly for the ternary system with hydrophobic or monohydroxyl nonsolvent systems; this was an indication of faster phase separation compared to the CA ternary systems with more hydrophilic nonsolvent systems (Table III and Figure S4 and S5, see Supporting Information). From Figure S5, it is clear that the change in η (slope) with increasing nonsolvent content was greater for the longer alkyl chain monohydric alcohols (Dec) as compared to Gly, PD, or Pro at high nonsolvent contents (>∼30 wt %). This was probably due to hydrophobic interactions, which led to phase separation and eventually solvent-phase partitioning of the system.

As shown in Figure 5, increasing the addition of PD, Gly, and Dec increased the respective average fiber diameter significantly. In fact, the CA/DMA/Dec system appeared to be primarily fibers, albeit some beaded fibrous structures were still evident. Similarly, an improvement in the fiber formation was observed for the CA/DMA/Oct ternary system, where a majority of fibers with some large droplets were observed. However, the increase in the solution η with the addition of Pro and Hex to their maximum content did not improve fiber formation, and spherical droplets were again obtained (Figure 5). This was significant

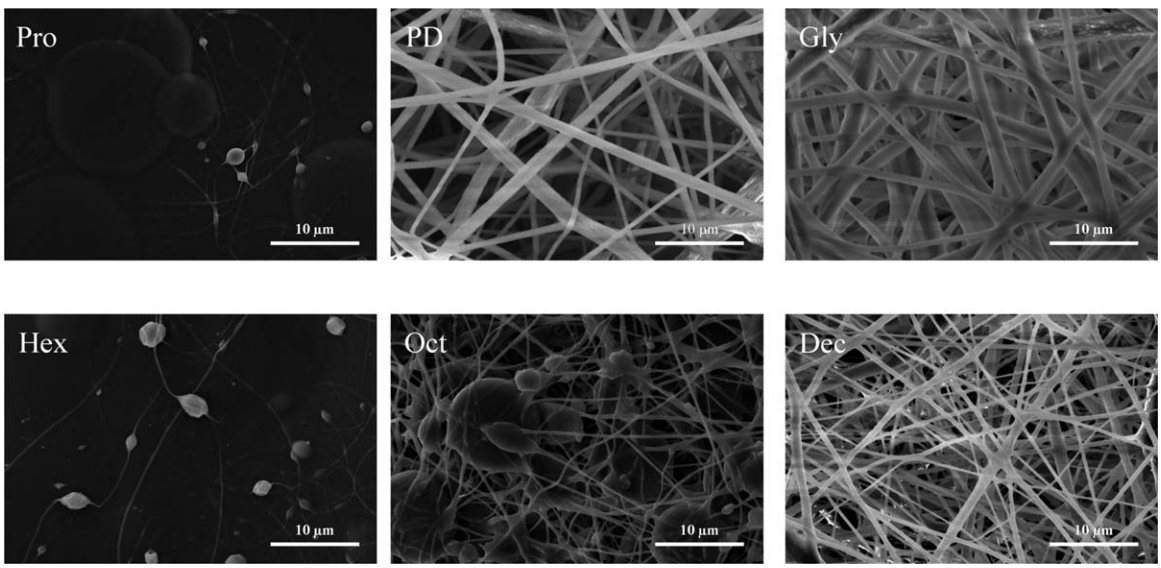

Figure 5. SEM micrographs of the electrospun CA fibers generated from ternary systems at the highest nonsolvent content (at the point before gelation) and with a CA content of 15 wt %.

Table IV. Hansen δs for the Components of the Various CA/DMA/Nonsolvent Ternary Systems

	δ ($MPa^{1/2}$)						
	δ_t	δ_d	δ_p	δ_h	χ	$D_{(S\text{-}p)}$	R
CA	25.1	18.6	12.7	11	—	—	12.4
DMA	22.9	16.8	11.5	10.2	0.17	7.52	—
Pro	22.7	15.6	6.7	15.3	0.18	45.2	—
Hex	21.9	15.7	3.9	12.6	0.24	55.3	—
Oct	19.8	16.5	3.1	11.2	0.41	58.9	—
Dec	19.2	16.0	2.6	10.2	0.45	64.8	—
PD	36.7	21.9	12.6	26.6	0.78	143.4	—
Gly	35.2	16.9	11.7	28.5	0.89	159.4	—

in that η of the CA/DMA/Hex system (9.6 Pa s at 40 wt % Hex) was higher than that of the CA/DMA/PD system (6.7 Pa s at 30 wt % PD), which formed uniform fibers (Table II and Figure 4). These results indicate that the electrospinning process for these ternary systems was mainly dominated by the structures of the nonsolvents and the number of hydroxyl groups present rather than the concentration of nonsolvents and the η of the CA ternary solution.

Effect of the Miscibility Parameters on Electrospinning

The differences in the solution properties and the resulting electrospun fiber morphology for all ternary systems were very much dependent on the intermolecular interactions between the solvent/nonsolvent and CA. As the strength of the intermolecular forces was equal to the cohesive energy density, the cohesive energy density values could be used to predict the solution behavior of CA in mixed solvent and nonsolvent systems. Typically, Hildebrand solubility parameters (δs), which are the square root of the cohesive energy density, are used to the predict solubility of polymers.[25–27] Here, we assumed that cohesive energy arose from the dispersive part of the solubility parameter (δ_d), permanent dipole–dipole part of the solubility parameter (δ_p), and hydrogen-bonding part of the solubility parameter (δ_h) forces where[25]

$$\delta^2 = \delta_d^2 + \delta_p^2 + \delta_h^2 \quad (1)$$

This three-term set represents different contributions to the free energy of the mixing, and the numerical value of the total solubility parameter (δ_t) demonstrates the relative solvency behavior of a solvent system for a specific polymer. Generally, complete miscibility is expected when δ_ts are similar between components in a mixture. Table IV summarizes the Hildebrand and Flory–Huggins parameters (χs) for each solvent and nonsolvent type in the ternary system. The calculated total solubility value for CA (δ_t) was shown to be 25.1, and on the basis of the corresponding values for the solvent/nonsolvent, the ability to dissolve CA decreased as follows: $\delta_{Pro} > \delta_{Hex} > \delta_{Oct} > \delta_{Dec} > \delta_{PD} > \delta_{Gly}$. χ was also used to characterize the polymer–solvent interactions, wherein a smaller value of χ indicated a more thermodynamically compatible interaction between the solvent and the polymer (Table IV). The Flory–Huggins interaction showed again that DMA was the most suitable solvent and that Gly had the least solubility for the CA polymer; this also confirmed the findings in our pervious study.[12]

An estimation of the spherical area of solubility for any specific polymer could be constructed in a three-dimensional coordinate system with δ_d, δ_p, and δ_h. The obtained radius of the polymer solubility Hansen sphere [$D_{(S\text{-}p)}$] is called the interaction radius (R). A polymer can be soluble in a solvent if the distance between the solvent and the center of $D_{(S\text{-}p)}$ is less than R for the polymer [$D_{(S\text{-}p)} < R$].[27,28] $D_{(S\text{-}p)}$ indicates the distance between the center of $D_{(S\text{-}p)}$ and the solvent. As shown in Table IV, the value of R or the spherical solubility area for CA was 12.40 $MPa^{1/2}$.[27] Accordingly, the calculated $D_{(S\text{-}p)}$ for DMA was less than R for the CA polymer, which was shown to be in the appropriate range for the dissolution of CA (Table IV). The calculated $D_{(S\text{-}p)}$ for the other individual nonsolvents was significantly greater than the R value of CA, where the greatest and least values were attributed to Gly and Pro, with values of 159.4 and 45.2 $MPa^{1/2}$, respectively. This supported the observed rapid (lowest concentration of nonsolvent required) phase separation of CA in the ternary systems with Gly as the nonsolvent.

Satisfactory electrospinning conditions can be established when polymers cross the phase boundary between solutions and solids. The kinetics of phase separation can, to a great extent, be attributed to the polymer concentration and the presence of other components, which aid in faster polymer solidification. In the electrospinning of the CA ternary systems, CA fiber formation was readily achieved when nonsolvents with greater $D_{(S\text{-}p)}$ values were used (e.g., Gly and PD). That is, a nonsolvent with a greater $D_{(S\text{-}p)}$ (Gly) could interact more with DMA, and as a result, faster CA phase separation via spinodal decomposition occurred. This led to rapid fiber formation. Conversely, satisfactory electrospinning conditions could not be established for the CA/DMA/Pro ternary system because of the poor performance of the DMA/Pro binary solvent system and its low $D_{(S\text{-}p)}$ of Pro, which was attributed to a delayed CA phase separation. As expected (Table IV), the calculated $D_{(S\text{-}p)}$ values were ranked such that Gly > PD > Dec > Oct > Hex > Pro and suggested the role of nonsolvents in initiating the sol–gel process; this was more significant in PD, Gly, and Dec. This suggests that these three nonsolvents were the least thermodynamically compatible

for dissolving CA, and therefore, the phase separation of CA was more greatly affected. As a result, during electrospinning, the phase changes or fiber formation of the CA polymer from the ternary systems with nonsolvents with high $D_{(S\text{-}p)}$ (PD and Gly) was greatly facilitated. This was supported by SEM analyses of the respective electrospun fibers, where the Dec, PD, and Gly ternary systems exhibited more uniform electrospun fibers than the others systems.

CONCLUSIONS

In this study, the impact of the solvent/nonsolvent structure and concentration on the CA ternary system solution properties and the morphology of CA electrospun products were thoroughly investigated. Various CA/DMA/nonsolvent ternary solutions were prepared with a range of nonsolvents, and their resulting electrospinning process were investigated. Increasing the CA content and nonsolvent concentration enhanced the rheological characteristics of the ternary system and facilitated the electrospinning process. Fiber formation and the average fiber diameter were shown to be highly dependent on the structure of the nonsolvent. Under optimal electrospinning conditions, both increasing the hydroxyl group content and hydrocarbon chain length of the nonsolvents improved fiber formation. For this ternary system, our findings demonstrate that the electrospinning process and fiber formation were mainly governed by the structure of the nonsolvent and the solution η. The calculated δs and $D_{(S\text{-}p)}$ values for the various components in our ternary system enabled the prediction of which CA ternary system would lead to fiber formation. The calculated $D_{(S\text{-}p)}$ values were ranked in the order of 7.5 (DMA) < 45.2 (Pro) < 55.3 (Hex) < 58.9 (Oct) < 64.8 (Dec) < 143.4 (PD) < 159.4 (Gly). Only the ternary systems with nonsolvents with high $D_{(S\text{-}p)}$ values (PD and Gly) showed the required fast phase separation of the CA polymer during electrospinning and resulted in smoother fiber formation. In future work, we will extensively discuss the effect of nonsolvents on the tensile strength, wet strength, and air and water filtration efficiency of the obtained electrospun fiber mats from all CA ternary systems.

ACKNOWLEDGMENTS

The authors greatly acknowledge the Sentinel Bioactive Paper Network and the Natural Sciences and Engineering Research Council of Canada for their financial support of this research.

REFERENCES

1. Heinze, T.; Liebert, T. *Macromol. Symp.* **2004**, *208*, 167.
2. Zuwei, M.; Kotai, M.; Ramakrishna, S. *J. Membr. Sci.* **2005**, *265*, 115.
3. Liu, H. Q.; Hsieh, Y. L. *J. Polym. Sci. Part B: Polym. Phys.* **2002**, *40*, 2119.
4. Saw, S. H.; Wang, K.; Yong, T.; Ramakrishna, S. In Tissue, Cell and Organ Engineering; Kumar, C. S. S. R., Ed.; Wiley-VCH: Weinheim, **2006**.
5. Li, W. J.; Laurencin, C. T.; Caterson, E. J.; Tuan, R. S.; Ko, F. K. *J. Biomed. Mater. Res. B* **2002**, *60*, 613.
6. Korehei, R.; Kadla, J. *Carbohydr. Polym.* **2014**, *100*, 150.
7. Korehei, R.; Kadla, J. *Biomacromolecules* **2011**, *12*, 43.
8. Ryskina, I. I. A.; Vysokomol, V. M. *Soedin. Ser. A* **1971**, *13*, 2189.
9. Matsuyama, H.; Nishiguchi, M.; Kitamura, Y. *J. Appl. Polym. Sci.* **2000**, *77*, 776.
10. Hao, J. H.; Wang, S. C. *J. Appl. Polym. Sci.* **2001**, *80*, 1650.
11. Ramakrishna, S.; Fujihara, K.; Teo, W.-E. An Introduction to Electrospinning and Nanofibers; World Scientific: Singapore, **2005**.
12. Korehei, R.; Kadla, J. *Biomacromolecules* **2010**, *11*, 1074.
13. Huang, Z. M.; Zhang, Y. Z.; Kotaki, M.; Ramakrishna, S. *Compos. Sci. Technol.* **2003**, *63*, 2223.
14. Bagherzadeh, R.; Latifi, M.; Najar, S. S.; Gorji, M.; Kong, L. *Text. Res. J.* **2012**, *82*, 70.
15. Bagherzadeh, R.; Shaikhzadeh Najar, S.; Latifi, M.; Kong, L. X. *J. Biomed. Mater. Res. A* **2013**, *101*, 2107.
16. Frenot, A.; Henriksson, M. W.; Walkenstrom, P. *J. Appl. Polym. Sci.* **2007**, *103*, 1473.
17. Filatov, Y.; Budyka, A.; Kirichenko, V. Electrospinning of Micro- and Nanofiber: Fundamentals and Applications in Separation and Filtration Processes; Begell House: New York, **2007**.
18. Tucker, N.; Stanger, J. J.; Staiger, M. P.; Razzaq, H.; Hofman, K. *J. Eng. Fibers Fabrics* **2012**, *7*, 63.
19. Anonymous. *Russ. J. Phys. Chem.* **2007**, *81*, 1355.
20. Golecki, H. M.; Yuan, H.; Glavin, C.; Potter, B.; Badrossamay, M. R.; Goss, J. A.; Phillips, M. D.; Parker, K. K. *Langmuir* **2014**, *30*, 13369.
21. Son, W. K.; Youk, J. H.; Lee, T. S.; Park, W. H. *J. Polym. Sci. Part B: Polym. Phys.* **2004**, *42*, 5.
22. Yun, S.; Chen, Y.; Nayak, J. N.; Kim, J. *Sens. Actuators B* **2008**, *129*, 652.
23. Tungprapa, S.; Puangparn, T.; Weerasombut, M.; Jangchud, I.; Fakum, P.; Semongkhol, S.; Meechaisue, C.; Supaphol, P. *Cellulose* **2007**, *14*, 563.
24. Andrady, A. L. Science and Technology of Polymer Nanofibres; Wiley: Hoboken, NJ, **2008**.
25. Hansen, C. M. *Svensk Kemisk Tidskrift* **1967**, *79*, 627.
26. Burrell, H. *J. Paint Technol.* **1968**, *40*, 197.
27. Hansen, C. Hansen Solubility Parameters: A User's Handbook, 2nd ed.; CRC: Boca Raton, FL, **2007**.
28. Burke, J. Solubility Parameters: Theory and Application; AIC Book and Paper Group Annual, Craig Jensen, eds., **1984**, *3*, 13.